Pis'ma v ZhETF, vol. 109, iss. 3, pp. 174 – 175

Vapor-phase synthesis and magnetoresistance of $(\mathrm{Cd}_{1-x}\mathrm{Zn}_x)_3\mathrm{As}_2$ ($x = 0.007$) single crystals

A. V. Kochura[a], *L. N. Oveshnikov*[b,c1)], *A. P. Kuzmenko*[a], *A. B. Davydov*[c], *S. Yu. Gavrilkin*[c], *V. S. Zakhvalinskii*[d], *V. A. Kulbachinskii*[b,e,f], *N. A. Khokhlov*[a], *B. A. Aronzon*[b,c]

[a] *Southwest State University, 305040 Kursk, Russia*

[b] *National Research Center "Kurchatov Institute", 123182 Moscow, Russia*

[c] *P.N. Lebedev Physical Institute, 119991 Moscow, Russia*

[d] *Belgorod National Research University, 308015 Belgorod, Russia*

[e] *Lomonosov Moscow State University, 119991 Moscow, Russia*

[f] *Moscow Institute of Physics and Technology (State University), 141700 Dolgoprudny, Russia*

Submitted 27 November 2018
Resubmitted 27 November 2018
Accepted 28 November 2018

DOI: 10.1134/S0370274X1903007X

Further advancement of modern technologies in many respects depends on the materials with fundamentally new properties. The Dirac and Weyl semimetals (DSM and WSM) are considered as such materials, having a tremendous potential for applications [1]. These semimetals have inverted band structure with a set of isolated Dirac points, where conduction and valence bands contact each other. The gapless electronic states near these symmetry-protected Dirac points have linear dispersion and rigidly coupled spin and momentum directions. The latter is characterized by their chirality ($C = \pm 1$). A DSM system, such as $\mathrm{Cd}_3\mathrm{As}_2$, have even number of Dirac points and doubly degenerate bands (chiral degeneracy). These systems are considered as a 3D graphene analogue, and therefore they are of considerable interest for both fundamental science and applications.

One of the difficulties in studies of $\mathrm{Cd}_3\mathrm{As}_2$ crystals is that the DSM features in it are often suppressed due to high bulk electron densities (related to high defect formation rate). There are four polymorphic modifications of the $\mathrm{Cd}_3\mathrm{As}_2$ lattice – α, α', α'', and β. Conventional melt crystallization techniques are not suitable for the growth of high-quality $\mathrm{Cd}_3\mathrm{As}_2$ single crystals due to the $\beta \to \alpha''$ phase transition, which leads to the formation of structural defects and to the increase in the charge carrier density. However, $\mathrm{Cd}_3\mathrm{As}_2$ crystals grown from the vapor phase at lower deposition temperatures demonstrate higher crystalline quality. The electron density in $\mathrm{Cd}_3\mathrm{As}_2$ can be diminished by a compensation doping, e.g., by Zn atoms [2, 3]. Crystals $(\mathrm{Cd}_{1-x}\mathrm{Zn}_x)_3\mathrm{As}_2$ form a continuous range ($0 \le x \le 1$) of solid solutions. The DSM-semimetal transition occurs at some doping level x_c. However, the data concerning the value of x_c are quite ambiguous. This stimulates further studies of corresponding transition and properties of $(\mathrm{Cd}_{1-x}\mathrm{Zn}_x)_3\mathrm{As}_2$ crystals. In this work we applied vapor-phase method to grow $(\mathrm{Cd}_{1-x}\mathrm{Zn}_x)_3\mathrm{As}_2$ single crystals. We investigated the structure, surface morphology and transport properties (for transverse, $B_\perp$, and longitudinal, $B_\parallel$, magnetic field orientations) of obtained samples. Here we present results for the sample with $x \approx 0.007$. This composition was confirmed by the energy-dispersive X-ray spectroscopy results (Zn – 0.42 at.%, Cd – 59.38 at.%, and As – 40.2 at.%).

The electron diffraction pattern for studied $(\mathrm{Cd}_{0.993}\mathrm{Zn}_{0.007})_3\mathrm{As}_2$ sample demonstrated high crystalline quality of the crystal and the absence of defects related to the Zn doping. The crystal lattice was found to be tetragonal with parameters $a = 12.7$ Å and $c = 25.4$ Å (which agrees well with $a = 12.6461$ Å and $c = 25.4378$ Å for α-$\mathrm{Cd}_3\mathrm{As}_2$ [4]). The surface of studied sample contain octahedron nuclei, which were earlier observed during the synthesis of $\mathrm{Cd}_3\mathrm{As}_2$ nanostructures from the vapor phase [5]. We also observed surface regions with pronounced step-like morphology, which, most likely, are formed by the {112} planes similarly to α-$\mathrm{Cd}_3\mathrm{As}_2$ single crystals [5, 6]. In the Raman spectrum of the sample, we observed two clearly pronounced peaks at 194 and 249 cm^{-1}, and a weak peak at 292 cm^{-1}. Similar patterns were observed for micro- and nanocrystals, as well as for single crystalline thin films of $\mathrm{Cd}_3\mathrm{As}_2$ at room temperature [7–10]. The 249 cm^{-1} and 292 cm^{-1} peaks, which we observed, do

1) e-mail: Oveshln@gmail.com

not correspond to the main oscillations of the lattice, but they are characteristic of the Cd_3As_2 and are usually associated with the presence of the defects (Cd vacancies) and with the scattering of individual phonons and collective plasmon modes by the Dirac electron system [11].

Magnetoresistance (MR) of $(Cd_{0.993}Zn_{0.007})_3As_2$ sample was measured at temperature $T = 4.2$ K for different magnetic field orientations and shown in Fig. 1.

We also observed clear Shubnikov–de Haas (SdH) oscillations. The background part of the transverse MR ($R(B_\perp)$) is linear for $B > 1$ T and rather huge (more than 150 %/T). The planar MR is non-linear and is about a half of the transverse MR. Linear MR in Cd_3As_2 crystals can appear due to weak inhomogeneities (such as As vacancies) leading to the fluctuations of carrier mobilites [12]. This model suggest that such MR should demonstrate only weak anisotropy. Thus, the observed substantial anisotropy of MR in studied $(Cd_{0.993}Zn_{0.007})_3As_2$ crystal is, most probably, due to a chiral anomaly, resulting in negative MR contribution [13]. The SdH oscillations also reveal pronounced anisotropy. Corresponding oscillations for the $B_\perp$ demonstrate only a single frequency, while oscillations for $B_\parallel$ reveal more complicated behavior. The latter is related to the presence of two oscillation frequencies as it is suggested by corresponding Fourier spectra (see inset in Fig. 1). This behavior is attributed to a possible nesting of the Fermi-surface ellipsoids at some crystallographic directions.

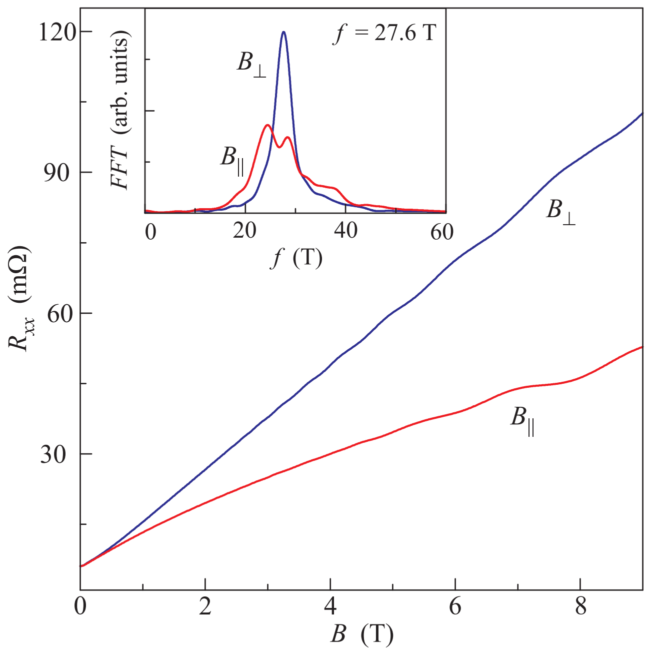

Fig. 1. (Color online) The MR curves for $(Cd_{0.993}Zn_{0.007})_3As_2$ sample measured at 4.2 K for different magnetic field orientations. Inset shows the Fourier spectra of Shubnikov–de Haas oscillations for two field orientations

From the temperature dependence of the SdH oscillation amplitudes we evaluated effective mass of charge carriers $m^* \approx 0.033m_e$ (m_e is the free electron mass) in the investigated $(Cd_{0.993}Zn_{0.007})_3As_2$ crystal. This value is in good agreement with $m^* \approx (0.023 \div 0.043)m_e$ found for undoped Cd_3As_2 crystals [12]. We also estimated corresponding electron density $n_{SdH} \approx 1.6 \times \times 10^{18}\,\mathrm{cm}^{-3}$, taking into the account the four-fold degeneracy of the Fermi surface in Cd_3As_2 crystal. Corresponding carrier mobility is about $5.5 \cdot 10^4\,\mathrm{cm}^2/(\mathrm{V \cdot s})$.

This work was partially supported by the Russian Science Foundation (grant # 17-12-01345). Raman spectroscopy studies, performed by A.P. Kuzmenko and N.A. Khokhlov, were partially supported by the Ministry of Education and Science of the Russian Federation (grant # 16.2814.2017/PCh).

Full text of the paper is published in JETP Letters journal. DOI: 10.1134/S0021364019030019

1. N. P. Armitage, E. J. Mele, and A. Vishwanath, Rev. Mod. Phys. **90**(1), 015001 (2018).
2. E. K. Arushanov, Prog. Crystal. Growth. Charact **25**(3), 131 (1992).
3. A. I. Belogorokhov, I. S. Zakharov, A. F. Knyazev, and A. V. Kochura, Inorganic Materials **36**(7), 653 (2000).
4. E. K. Arushanov, Prog. Crystal. Growth. Charact. **3**(2–3), 211 (1981).
5. C.-Z. Li, R. Zhu, X. Ke, J.-M. Zhang, L. X. Wang, L. Zhang, Z.-M. Liao, and D.-P. Yu, Cryst. Growth Design **15**(7), 3264 (2015).
6. M. N. Ali, Q. Gibson, S. Jeon, B. B. Zhou, A. Yazdani, and R. J. Cava, Inorganic Chemistry **53**, 4062 (2014).
7. P. Schonher and T. Hesjedal, Appl. Phys. Lett. **106**(1), 013115 (2015).
8. K. Zhang, H. Pan, M. Zhang, Z. Wei, M. Gao, F. Song, X. Wang, and R. Zhang, RSC Advances **7**(29), 17689 (2017).
9. P. Cheng, C. Zhang, Y. Liu, X. Yuan, F. Song, Q. Sun, P. Zhou, D. W. Zhang, and F. Xiu, New J. Phys **18**(8), 083003 (2016).
10. A. V. Kochura, S. F. Marenkin, A. I. Ril, A. L. Zheludkevich, P. V. Abakumov, A. F. Knjazev, and M. B. Dobromyslov, J. Nano Electron. Phys. **7**(4), 04079 (2015).
11. A. Sharafeev, V. Gnezdilov, R. Sankar, F. C. Chou, and P. Lemmens, Phys. Rev. B **95**(23), 235148 (2017).
12. A. Narayanan, M. D. Watson, S. F. Blake, N. Bruyant, L. Drigo, Y. L. Chen, D. Prabhakaran, B. Yan, C. Felser, T. Kong, P. C. Canfield, and A. I. Coldea, Phys. Rev. Lett. **114**(11), 117201 (2015).
13. H. Li, H. He, H.-Z. Lu, H. Zhang, H. Liu, R. Ma, Z. Fan, S.-Q. Shen, and J. Wang, Nature Comm. **7**, 10301 (2016).